Searches for Minimal Supersymmetry at HERA

Peter Schleper

Physikalisches Institut, Universität Heidelberg
and
CERN-PPE, Geneva
Peter.Schleper@cern.ch

Abstract: The potential for the discovery of particles predicted by the minimal supersymmetric standard model in a future, high luminosity run of HERA is investigated. For the most promising process of selectron and squark production, the kinematic analysis shows that a supersymmetric signal can be found free of background from standard model processes. If however no signal would be found, selectrons and squarks can be excluded up to $(M_{\tilde{e}}+M_{\tilde{q}})/2 \lesssim 100$ GeV for a large part of the SUSY parameter space. This number assumes that an integrated luminosity of 250 pb^{-1} will be collected by both experiments and that the experimental results are combined. This search is in many aspects complementary to the potential yield at LEP II and the TEVATRON.

1 Introduction

Supersymmetry (SUSY) is presently considered to be the most promising candidate for an extension of the standard model (SM). While there is strong theoretical motivation for the existence of this new fundamental symmetry of nature, there is as yet no convincing experimental evidence for the new particles predicted. For an introduction to the SUSY particle spectrum and the corresponding literature see [1].

In the following the discussion is restricted to the minimal supersymmetric standard model (MSSM), which is defined by having minimal particle content in addition to the SM and minimal additional interactions, i.e. it will be assumed that R-parity [1] is conserved. It is generally assumed that the lightest SUSY particle (LSP) is the lightest neutralino χ_1^0. R-parity conservation implies that the LSP is stable and that SUSY particles can only be produced in pairs. Since the initial state at an ep collider, namely $e+q$ or $e+g$, does not easily allow for pair productions of new particles, the search for minimal SUSY at HERA is limited to only very few processes:

- $eq \to \tilde{e}\tilde{q}$. This is the most promising channel and will be analysed here (see Fig. 1). A similar analysis using the presently available data of H1 was published in [2]. The same process, however with the assumption that R-parity is broken, was analysed in [3].
- $eq \to \tilde{\nu}\tilde{q}'$. Experimentally this process has a less distinct signature, and an irreducible background from charged current events.

- $eq \to eq\tilde{g}\tilde{g}$ for light gluinos. This channel is difficult to distinguish from SM multi-jet events as discussed in [4].
- $eq \to \tilde{e}\chi_1^0 q$. This channel has a rather small cross section and does not allow a discovery [5].

Any SUSY search depends in detail on the numerous new parameters of the MSSM, or on theoretical assumptions for relations between these parameters. In the following, two different scenarios will be evaluated:

MSSM with no additional constraints: For this analysis, the relevant free parameters of this model are the gaugino mass parameters M_1 and M_2, the parameters of the Higgs sector $\tan\beta$ and μ, and the sfermion masses of $\tilde{f}_L, \tilde{f}_R$, where f stands for e, ν_e, u, d, s, c.

MSSM with constraints from GUT models: Here only one common scalar mass m_0 and one common gaugino mass $m_{1/2}$ are relevant together with $\tan\beta$ and $sign(\mu)$. The assumptions motivated by GUT models are used to derive all other masses via renormalisation group equations (RGE), which results in strong correlations between the masses of SUSY particles.

For the general discussion of kinematics, cross sections etc. the unconstrained model will be used. For the sake of simplicity all numerical results are derived assuming equal masses for the partners of left and right handed fermions. Also the squark masses of the first two generations are assumed to be equal. Further, all calculations are done with a value of $M_1 = (5/3)\tan^2\theta_W \; M_2$ where θ_W is the weak mixing angle. This is in fact motivated by GUT models. Relaxing these assumptions will not modify the main conclusions, as will be discussed. In section 7 the constrained model is treated. It will always be assumed that gluinos are heavier than squarks.

The most promising SUSY process at HERA is the interchange of a supersymmetric neutralino between the beam electron and a quark of the proton as shown in Fig. 1. The

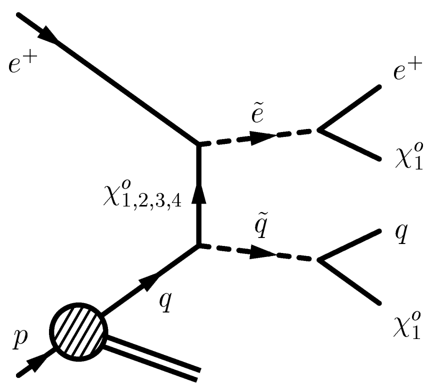

Figure 1: *Feynman diagram for selectron - squark production via neutralino exchange and the subsequent decays into the lightest supersymmetric particle LSP.*

final state consists of a selectron and a squark. These sfermions decay into their SM partners and gauginos. The signature of the process is therefore an electron, a jet and 2 gauginos. In the experimentally most favourable case, these gauginos are χ_1^0's. They leave the apparatus undetected and therefore can be tagged by requiring missing energy and momentum. Depending in detail on which part of the MSSM parameter space is investigated, decays into other gauginos are possible or even dominant. These are much more difficult to detect and will not be considered at this stage. In any case it is crucial to take the full dependence on the MSSM parameters into account for the interpretation of the experimental results.

2 The event generator HERASUSY

For the determination of numerical results an event generator (HERASUSY) was written. This generator was also applied for the analysis in [2]. The program makes use of the ISASUSY package [7] for the investigation of the SUSY parameter space. In the context of HERASUSY, the ISASUSY package is mainly used to calculate from the basic SUSY parameters the mass eigenstates of neutralinos and the branching ratios of sfermions into gauginos. For the evaluation of the constrained MSSM, the routines ISASUGRA from the ISASUSY package are applied. These allow to calculate from the parameters $m_0, m_{1/2}$ etc. the low energy SUSY masses and couplings by making use of the second order RGEs.

From the results of ISASUSY or ISASUGRA, the couplings between neutralinos and sfermions are determined, which enter in the cross section calculation. The differential cross section for the neutralino exchange diagrams and their interference was derived in [6]. This calculation includes the full dependence on the free parameters of the unconstrained MSSM. The integration of this cross section and random generation of events in x and Q^2 is done using the programs BASES and SPRING. The results on the total cross section are found to be in reasonable agreement with those in [6].

Routines for the kinematics of sfermion decays into fermions and the χ_1^0 are added. The whole package is interfaced to PYTHIA [8] in order to allow for parton showers and fragmentation. The output of PYTHIA is available in a format suitable for simulations with the standard, GEANT–based detector simulation of the H1 detector, which was applied for all distributions shown.

In order to allow a detailed investigation of the MSSM parameter space the package can be steered such that loops on the MSSM parameters, constrained or unconstrained, are performed. For each new set of parameters the cross section is calculated and events are generated, if desired.

The program is available on request from the author.

3 Cross Section and Branching Ratios

The sensitivity of the HERA experiments depends on the cross section for $\tilde{e}$-$\tilde{q}$ production, the branching ratios into different gauginos and how well the corresponding signals can be detected. Each of these ingredients depends in a non-trivial way on the basic SUSY parameters as defined in section 1.

Concerning the cross section, the exchange of neutralinos in the t-channel is completely analogous to deep inelastic scattering (DIS) in the SM, where γ and Z^0 are exchanged. The main difference is that potentially very heavy particles have to be produced. This means first of all, that the invariant mass of the incident electron and quark has to be larger than the kinematic threshold for $\tilde{e}$-$\tilde{q}$ production,

$$(e + xp)^2 = x\,s > (M_{\tilde{e}} + M_{\tilde{q}})^2, \tag{1}$$

where x denotes the momentum fraction of the quark in the proton and e and p denote the 4-vectors of the beam particles. Due to the steep fall of the quark distribution function towards large x this determines the main dependence of the cross section on the SUSY parameters. Also the 4-momentum transfer Q^2 between the beam electron and the $\tilde{e}$ has to be larger than

$$Q^2 > \frac{1}{2}\left\{ xs - M_{\tilde{e}}^2 - M_{\tilde{q}}^2 - \sqrt{\left(xs - M_{\tilde{e}}^2 - M_{\tilde{q}}^2\right)^2 - 4M_{\tilde{e}}^2 M_{\tilde{q}}^2} \right\}. \tag{2}$$

In this supersymmetric process four neutralinos $\chi^0_{1,2,3,4}$ can be exchanged. Their amplitudes interfere, similar to the interference of γ and Z^0 in standard DIS processes. The relative contribution of the $\chi^0_{1,2,3,4}$ depends on the strength of their couplings to fermions and on the neutralino masses. Because the neutralinos are the mass eigenstates of a mixing matrix of $\tilde{\gamma}$, $\tilde{Z}$ and neutral higgsinos, their couplings are derived from the parameters entering this mixing matrix. If a neutralino has a strong higgsino component (i.e. $M_2 << |\mu|$), it couples only extremely weakly to the electron and the light quarks in the proton. In this case this neutralino does not contribute significantly to the cross section. In the other cases, when the $\tilde{\gamma}$ or $\tilde{Z}$ components are large (for $\mu << -M_2$ or $\mu >> M_2$), the couplings are of the same magnitude as for the γ or Z^0.

The dependence of the χ^0_1 and $\chi^\pm_1$ masses on the MSSM parameters is shown in Fig. 2. For a given set of parameters the LSP is considerably lighter than the lightest chargino.

The neutralino masses $m_{1,2,3,4}$ for $\chi^0_{1,2,3,4}$ enter in the propagator term of the cross section in the form

$$\sigma \sim \sum_{i,j=1}^{4} \frac{C_{ij}}{(Q^2 + m_i^2)(Q^2 + m_j^2)} \tag{3}$$

where the interference between the four exchange diagrams is already taken into account. C_{ij} denotes products of the couplings of neutralino i and j to fermions as discussed above. Due to the potentially large mass differences the most important contribution is expected from the lightest supersymmetric particle, the LSP. If however the LSP is higgsino like, the χ^0_2 will most often give the largest contribution. In this case the cross section is very much reduced since the leading part of the propagator sum in the equation above is much smaller, and often too small for a measurement.

Also the branching ratios of the $\tilde{e}$ and $\tilde{q}$ depend on the neutralino couplings and masses. In the simplest case, the $\tilde{e}$ and $\tilde{q}$ decay only into the χ^0_1 and e, q, respectively. This is the case when the χ^0_1 is lighter than $\tilde{e}$ and $\tilde{q}$, and all other gauginos are heavier such that decays into them are kinematically forbidden. If also other gauginos, first of all χ^0_2 and $\chi^\pm_1$, are light enough (and not higgsino–like), then decays into these particles will generally contribute considerably, and the branching ratios into the χ^0_1 are correspondingly reduced.

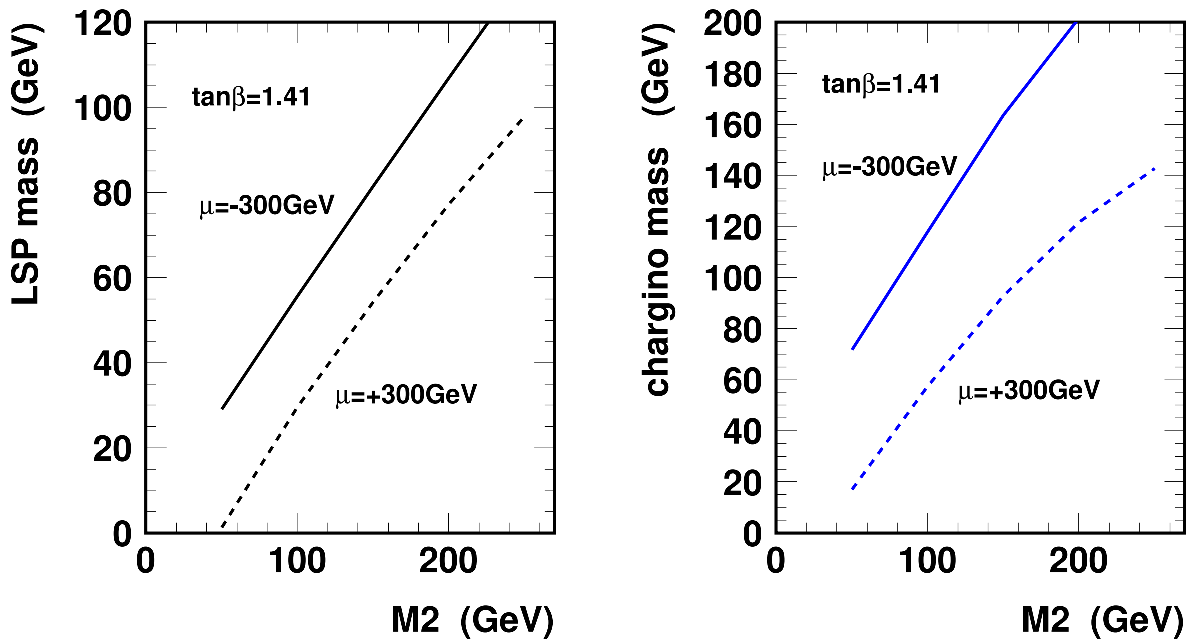

Figure 2: *Masses for the lightest neutralino (LSP) and the light chargino $\chi_1^\pm$ in dependence of other MSSM parameters.*

Experimentally, the two decay modes of sfermions, $\tilde{f} \to f\chi_1^0$ and $\tilde{f} \to f\chi$ (where $\chi = \chi^0_{1,2,3,4}, \chi^\pm_{1,2}$) have very different characteristics. The χ_1^0 is absolutely stable in the MSSM, because it is the lightest SUSY particle, and cannot be measured in the detector. The signature of an χ_1^0 is therefore missing energy or momentum. This is the gold plated signature for supersymmetry, for which searches have been performed at all colliders.

The other gauginos undergo decays into matter fermions and lighter gauginos, $\chi_m \to f\bar{f}'\chi_n$, where $f\bar{f}'$ are pairs of matter fermions and $\chi_{m,n} = \chi^0_{1,2,3,4}, \chi^\pm_{1,2}$ with $M_{\chi_m} > M_{\chi_n}$. In fact a cascade of decays to lighter and lighter gauginos occurs with the χ_1^0 as the final particle. This leads to multi–fermion final states, which are generally more difficult to identify than the direct decay $\tilde{f} \to f\chi_1^0$. Also the momentum of the χ_1^0's from cascade decays are smaller than from the direct decay, which leads to less striking signals.

In the analysis presented here, and also in the published analysis of H1 [2], cascade decay modes have been taken into account as a change of the branching ratio $BR(\tilde{f} \to f\chi_1^0)$, but have not been searched for directly.

In Fig. 3 the cross section for $\tilde{e}$-$\tilde{q}$ production times the branching ratios $BR(\tilde{e} \to e\chi_1^0)$ $BR(\tilde{q} \to q\chi_1^0)$ is shown, as obtained from HERASUSY. Given is the dependence on the sum of the $\tilde{e}$ and $\tilde{q}$ masses, $(M_{\tilde{e}} + M_{\tilde{q}})/2$, which reflects the kinematic threshold for this process. Beside phase space effects and branching ratios, the slope of the curves is mainly driven by the drop of the quark density functions in the proton towards large x. For the value of the higgsino mass parameter μ two extreme cases are shown. For $\mu = -500$ GeV the χ_1^0 is $\tilde{\gamma}$–like and for $\mu = +500$ GeV it is $\tilde{Z}$–like. The cross sections are not very different and range from about 1pb at $(M_{\tilde{e}} + M_{\tilde{q}})/2 \approx 60$ GeV to about 0.01pb for $(M_{\tilde{e}} + M_{\tilde{q}})/2 \approx 100$ GeV. The cross sections have been obtained for $\tan\beta = 1.41$ as an example for a low value for $\tan\beta$, $M_2 = 100$ GeV and $M_1 = 50$ GeV. These values lead to $M_{\chi_1^0} = 55$ GeV (30 GeV) and $M_{\chi_2^\pm} = 117$ GeV (55 GeV) for $\mu = -300$ GeV (+300 GeV),

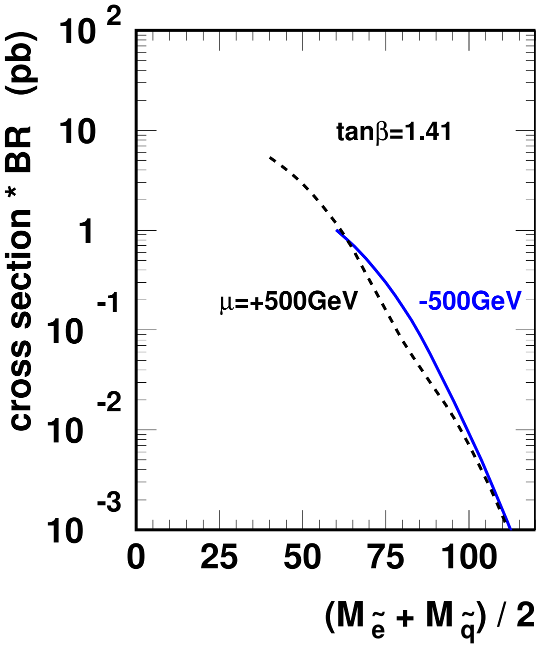

Figure 3: *Cross section times branching ratios for selectron-squark production and subsequent decays into the χ_1^0 at HERA.*

respectively. For the envisaged integrated luminosity of up to 500 pb^{-1}, these are still reasonable cross sections.

4 Background Rejection

The most important background processes are those which either lead to electron candidates or to neutrinos, since these would fake the unmeasured χ_1^0's, namely DIS neutral and charged current events and W decays into $e\nu$. The following cuts are suitable to reject these backgrounds, and illustrated in Fig. 4:

- The polar angle θ_e of the electron should be in the range $20^o < \theta_e < 130^o$, where the upper bound is used to reduce the NC background. The lower bound ensures that the charged track of the electron is measured in the central tracking detector. This requirement is used mainly to reject CC events with radiative γ's, which cannot be rejected otherwise and would have led to an irreducible background of 29 expected events for 500 pb^{-1} after all cuts.
- The quark polar angle θ_q as predicted by the measured electron must be larger than 20^o in order to avoid large missing transverse momentum $P_{T,miss}$ induced by leakage in the beam pipe. This is the most important contribution to $P_{T,miss}$ in neutral current events as shown in Fig. 4 a), where at small θ_q a tail towards positive values of the net transverse momentum of the event parallel to the electron indicates a loss of hadronic energy.
- The $E - P_z$ value of the entire event has to be below 30 GeV. For $\tilde{e}$-$\tilde{q}$ events this small value (when compared to the nominal value of twice the electron beam energy) is due to the unmeasured χ_1^0's. For NC events this means that only events with hard initial state radiation remain as background.

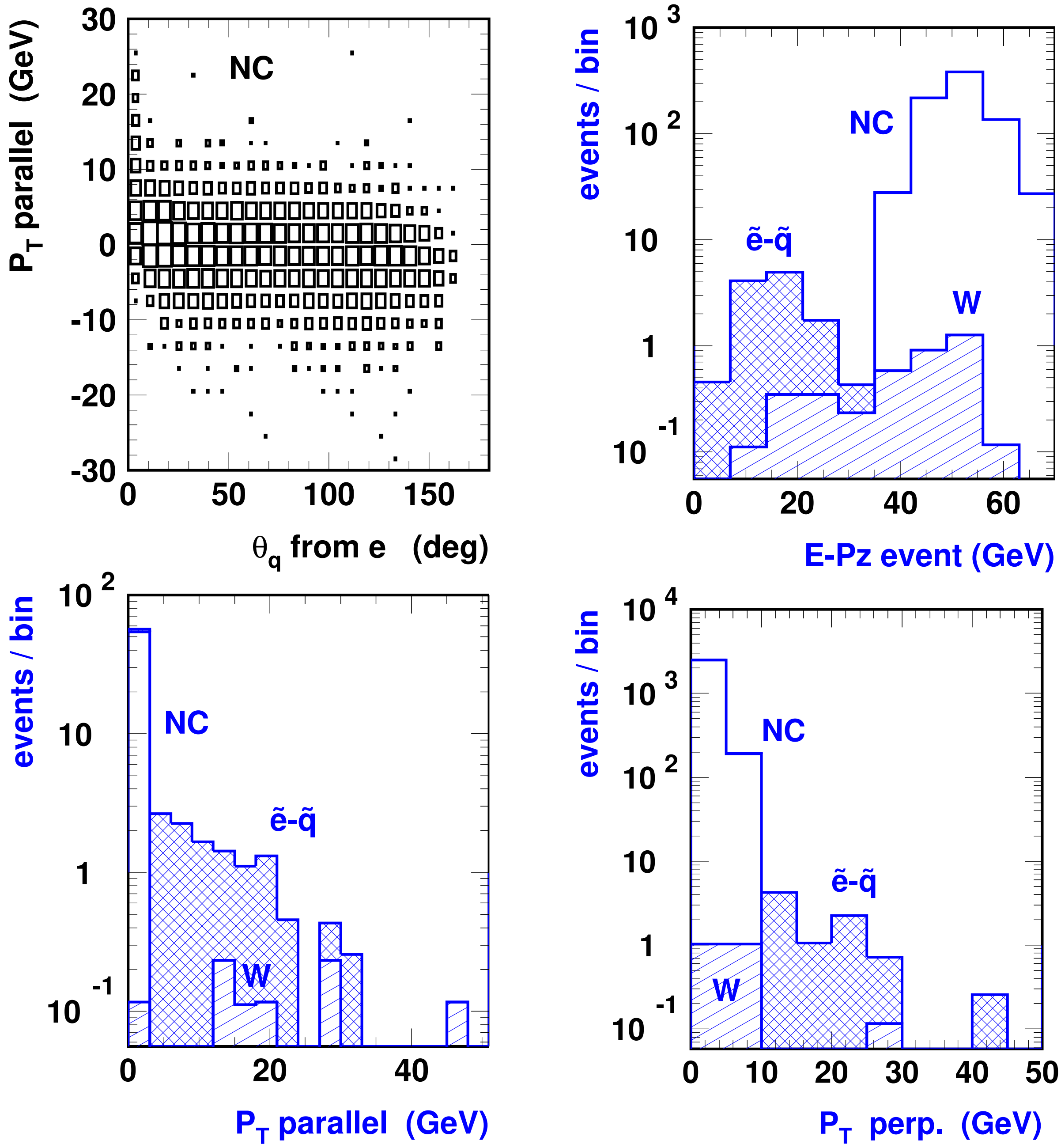

Figure 4: *Kinematic quantities from monte carlo event samples used for the $\tilde{e}$-$\tilde{q}$ search: a) Component of the event P_T vector parallel to the electron versus the quark polar angle calculated from the electron for neutral current events (NC). The size of the boxes is proportional to the logarithm of the number of events. b) E-Pz distribution for W events with decays into $e + \nu$, and added to this the contribution from NC and $\tilde{e}$-$\tilde{q}$ events ($M_{\tilde{e}} = M_{\tilde{q}} = 80$ GeV, $M_{\chi_1^0} = 60$ GeV). c) and d) Distributions of the event P_T vector parallel and perpendicular to the electron for the same monte carlo events. All distributions are normalised to a luminosity of 500 pb^{-1}.*

- The $P_{T,miss}$ vector components perpendicular (parallel) to the electron momentum direction has to exceed 7 (3) GeV. These small values are necessary for a good efficiency for the signal. However they impose a major challenge for the understanding of the detector calibration and of tails in the experimental resolution for $P_{T,miss}$. In the published analysis [2] similar cuts were used and turned out to be feasible.
- The electron energy has to be smaller than 40 GeV. This suppresses W decays by about a factor 2, while for small mass differences between χ_1^0 and $\tilde{e}$,$\tilde{q}$ the efficiency loss is marginal.

In Fig. 4 b,c,d), the distributions for $E - Pz$ and the $P_{T,miss}$ vector components parallel and perpendicular to the electron directions are shown after full detector simulation. All cuts mentioned above have been applied, with the exception of the cut on the quantity which is shown in the figure. The background from W decays into $e\nu$ is given as a hatched histogram. Added on this is the NC contribution (open hist.) and the expected signal for $\tilde{e}$-$\tilde{q}$ production (crossed hist.). All distributions are normalised to an integrated luminosity of 500 pb^{-1}. For the SUSY signal, $\tilde{e}$ and $\tilde{q}$ masses of 80 GeV and a $\tilde{\gamma}$–like χ_1^0 with a mass of 60 GeV were chosen as an example. The cross section in this case is $\approx$ 0.1pb, which means that for the achieved efficiency of 22% more than 10 candidate events are expected. The huge NC background falls rapidly for the quantities shown and is completely suppressed by the cuts. In all distributions the signal is easily recognised. The only remaining background origins from W production and amounts to 0.16 events for W^+ and W^- together. This good suppression is here mainly achieved by the cut on the perpendicular component of P_T, and to a lesser extend also due to the cuts on electron energy and angle.

The efficiency of this search depends on the visible energy of the decay products of $\tilde{e}$-$\tilde{q}$, which can be parameterised as a function of the mass differences $M_{\tilde{e}} - M_{\chi_1^0}$ and $M_{\tilde{q}} - M_{\chi_1^0}$ (for details see [2]). They range from 20 to 25% for $M_{\tilde{e},\tilde{q}} - M_{\chi_1^0}$ >15 GeV. At smaller mass differences the efficiency drops rapidly and reaches 5% (1%) for mass differences of 10 GeV (5 GeV). The dependence on all other MSSM parameters is very weak in comparison, since these do not influence the final state kinematics significantly. The systematic errors due to the knowledge of the parton density functions, energy calibration and background estimation modify the final results typically by less than 2 GeV. This does not include theoretical uncertainties in the cross section calculation due to higher order effects.

In conclusion a signal for $\tilde{e}$-$\tilde{q}$ production could be found basically without background contamination, as long as the mass difference between $\tilde{e}$ and χ_1^0 and also $\tilde{q}$ and χ_1^0 is larger than $\approx$ 15 GeV.

5 Results for the unconstrained MSSM

For the derivation of possible bounds, a systematic survey of the MSSM parameter space was performed. Within the unconstrained MSSM described in section 1, the parameters $M_{\tilde{e}}$, $M_{\tilde{q}}$, and M_2 were varied independently within the bounds $45 < M_{\tilde{e}}, M_{\tilde{q}} < 160$ GeV and $0 < M_2 < 200$ GeV. This was done for values of μ of -300 and +300 GeV, corresponding to a $\tilde{\gamma}$–dominated and $\tilde{Z}$–dominated χ_1^0. As argued in section 3, a higgsino–dominated χ_1^0 is not accessible at HERA. The values chosen for $\tan\beta$ are 1.41 and 35. For other

MSSM parameters see section 1. The results for $\tan\beta$ =1.41 and μ=-300 GeV are presented in Fig. 5. Shown is the excluded region of $(M_{\tilde{e}} + M_{\tilde{q}})/2$ versus the gaugino mass

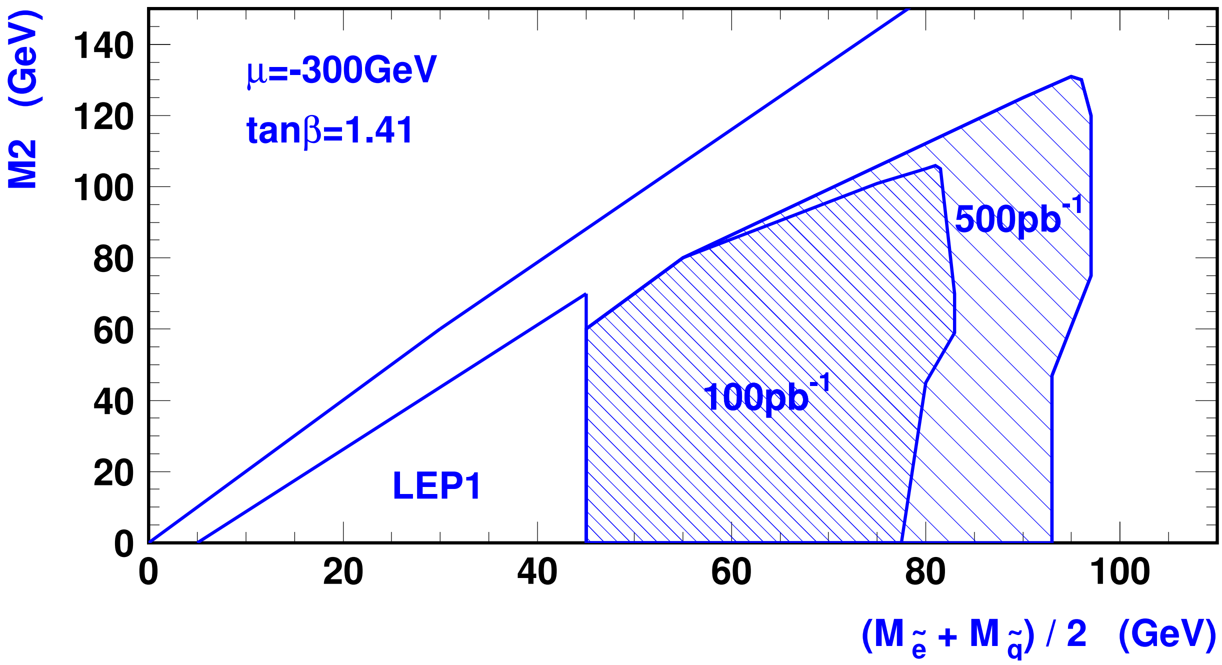

Figure 5: *Exclusion limits from HERA for $\tilde{e}$-$\tilde{q}$ production. Shown are areas which could be excluded at 95% CL for an integrated luminosity of 100* pb^{-1} *and 500* pb^{-1}*. Also shown is the region excluded by LEP 1.*

parameter M_2. The hatched areas correspond to an integrated luminosity of 100 pb^{-1} respectively 500 pb^{-1} of both experiments together , assuming that no candidates are found. The highest masses accessible are 130 GeV for M_2, and up to 100 GeV for $(M_{\tilde{e}} + M_{\tilde{q}})/2$. The shape of the excluded domain can be understood as follows:

The diagonal line is the limit where the χ_1^0 has the same mass as the $\tilde{e}$ or $\tilde{q}$. The region very close to this line cannot be explored because for small mass differences, the remaining energy for the final state e and q of the decays $\tilde{e} \to e\chi_1^0$ and $\tilde{q} \to q\chi_1^0$ becomes too small. Also the cross section is smaller for large χ_1^0 masses.

The maximum range for $(M_{\tilde{e}} + M_{\tilde{q}})/2$ is limited by the available energy in the initial eq system. The drop of the quark density function towards large x (roughly $\sim (1-x)^3$) is compensated by an increase of the integrated luminosity. It should be noted that the highest energy reached in the figure, namely $M_{\tilde{e}} + M_{\tilde{q}} \approx 190$ GeV, is still considerably below the maximum possible reach of $\sqrt{s} = 300$ GeV. Therefore an even higher luminosity than 500 pb^{-1} is certainly desirable.

At small values of the gaugino mass parameter M_2 the sensitivity for $(M_{\tilde{e}} + M_{\tilde{q}})/2$ is slightly reduced because also decays into other gauginos start to become allowed kinematically.

Parameter Dependence In [2] it has been shown that the dependence on μ is negligible if the higgsino–component of the χ_1^0 is small. The result therefore applies as long as $\mu \lesssim M_2$. A higgsino–like χ_1^0 is not accessible at HERA. For a $\tilde{Z}$–like χ_1^0 the bounds on $M_{\tilde{e},\tilde{q}}$

are about 10 GeV higher than shown in Fig. 5 (see however the discussion of the bounds from LEP2 below).

The choice of $\tan\beta$ influences only very little the cross section and the values chosen here are preferred theoretically and close to those obtained from global fits of SUSY parameters to data [9]. For $\tan\beta = 35$, the bound on M_2 is about 10 GeV higher than for $\tan\beta = 1.41$.

M_1 was related here to M_2 only because this allows a straight forward comparison with LEP2 results. For a $\tilde{\gamma}$–like χ_1^0, the limits depend however more directly on the χ_1^0 mass, because this enters in the propagator term of the cross section and the efficiency. The dependence on M_1 and M_2 is to first approximation given only indirectly through this dependence on the χ_1^0 mass, and can be deduced from Fig. 2 and Fig. 5. Therefore the relation $M_1 = (5/3)\tan^2\theta_W\ M_2$ can be relaxed without a major change of the result, as long as the χ_1^0 mass remains constant and the χ_1^0 is $\tilde{\gamma}$–like. Also the other neutralinos have to be heavy enough so that their contribution to the cross section is small. This means that M_2 could be much higher than actually shown in Fig. 5.

The assumption was made that the SUSY partners of left and right handed fermions have the same mass. If this is not the case the cross section would be reduced. In the extreme case that for example both $\tilde{e}_L$ and $\tilde{q}_L$ are much heavier than $\tilde{e}_R$ and $\tilde{q}_R$, the cross section would be reduced by more than a factor two, as can be verified from [6]. Fig. 3 shows that this would lead to mass bounds about 5 GeV (at most 10 GeV) lower than the ones displayed in Fig. 5.

6 Comparison with LEP and TEVATRON

At the time when the HERA experiments will have achieved the luminosities shown in Fig. 5, the LEP2 collider will presumably run at ≈ 190 GeV, and the main injector at the TEVATRON is expected to deliver a luminosity of 1000 pb^{-1} per year. The searches at both colliders will be close to their maximum reach when the HERA upgrade becomes effective.

Chargino Searches at LEP2: A mass of the $\chi_1^\pm$ close to $E_{\text{cms}}/2$=95 GeV can be tested [10]. For a $\tilde{\gamma}$–like χ_1^0 ($\mu = -300$ GeV), this corresponds to $M_2 = 75$ GeV as can be seen from Fig. 2. The HERA sensitivity is much better in comparison and reaches up to 130 GeV. In addition the LEP2 bounds will be weaker if the $\tilde{\nu}$ mass is small. In contrast, for a $\tilde{Z}$–like χ_1^0 the LEP2 bound of $M_2 = 155$ GeV is stronger than the HERA bound.

$\tilde{e}$ and $\tilde{q}$ searches at LEP2: Also here, mass limits close to the kinematic boundary for pair production can be achieved provided the integrated luminosity is high enough [10]. The resulting bound is therefore almost identical to the one reachable at HERA. In case of a discovery the combination of the results will allow important checks because the production mechanisms depend in a different way on the MSSM parameters.

$\tilde{q}$ **searches at the TEVATRON:** Already now the TEVATRON experiments have set limits for $\tilde{q}$ masses of several hundred GeV, which however depend on the values assumed for the χ_1^0 and gluino masses and on theoretical assumptions [11]. The HERA results in contrast are independent of the $\tilde{g}$ mass.

- In [11] no bounds on $M_{\tilde{q}}$ could be set within the *constrained* MSSM for $M_{\tilde{g}} \gtrsim 500$ GeV. This is partially due to the inclusion of cascade decays, to the connection of $M_{\tilde{g}}$ to $M_{\chi_1^0}$ in GUT models, and to a reduced sensitivity if $M_{\chi_1^0}$ is close to $M_{\tilde{q}}$.

  This result cannot be translated directly into the different theoretical assumptions made in this paper, because the masses of gauginos, the squark branching ratios and the significance of the $P_{T,miss}$ signal from χ_1^0's differ considerably.

- In [11] high bounds on $M_{\tilde{q}}$ were set within the *unconstrained* MSSM independently of the gluino mass, however only for $M_{\chi_1^0} < 15$ GeV and assuming that there are no cascade decays. The HERA bounds in comparison extend up to about $M_{\chi_1^0}$ =60 GeV.

The TEVATRON certainly has a larger potential for $\tilde{q}$ searches than HERA. On the other hand also the QCD background is much larger. This means that the HERA results will only be competitive in that part of the parameter space where the mass difference between $\tilde{q}$ and χ_1^0 is very small. In this case the jets from squark decays into the χ_1^0 have rather low energies and also the missing P_T signal is degraded. This signature is probably much more difficult to find at the TEVATRON than the $e + q + P_{T,miss}$ signal at HERA. For example this analysis uses a $P_{T,miss}$ threshold of less than 10 GeV, and is sensitive to mass differences as small as 20 GeV.

In conclusion, the HERA results will be competitive to those from LEP for a $\tilde{\gamma}$–like χ_1^0. In comparison to TEVATRON the only gap, if existing, would be for a χ_1^0 mass close to the $\tilde{q}$ mass.

7 Results for the Constrained Supersymmetric Model

Using the procedure described in section 2 the cross section for $\tilde{e}$–$\tilde{q}$ production was evaluated for many combinations of m_0 and $m_{1/2}$, positive and negative μ and $\tan\beta$ =1.41 and 35. Only those parameter sets were accepted which obey constraints from the measurement of the Z^0 width, from grand unification and electroweak symmetry breaking. In comparison to Fig. 3 only small differences were found due to the mass splittings in the fermion sector. However, as expected, the limits for $M_{\chi_1^0}$ and $M_{\tilde{q}}$ as shown in Fig. 5 also lead to limits on the gluino mass, since these quantities are related to each other via the RGEs. In comparison to the TEVATRON bounds [11] obtained already now with the same theoretical assumptions, the gluino mass limits obtained for HERA were found to be smaller for all parameter combinations tested. From this it is concluded that HERA also with high luminosity can not improve on present bounds for this model.

8 Detector Modifications for High Luminosity Runs

The envisaged upgrade of HERA implies severe changes to the detectors, the most important being that new magnets are inserted very close to the vertex. These will not disturb the central track measurements, but in front of the calorimeters and at polar angles below 80mrad, a large amount of material will be added. The expected effects for new particle searches are the following:

- The acceptance for particles at low angles is reduced. For the production of heavy new particles this could cause problems because these are always boosted into the forward direction due to the large mismatch between the beam energies at HERA. As it is shown however in Fig. 6 this turns out to be no problem. For a heavy

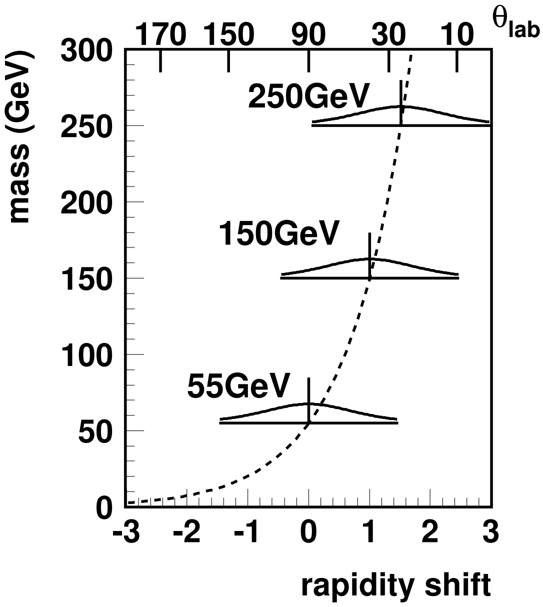

Figure 6: *Mean rapidity boost for decay products of heavy particles (dashed line). Overlayed are for three different masses the rapidity distributions of decay products, assuming an isotropic 2-body decay.*

  particle A of mass M_A produced via $ep \to AX$, the rapidity boost δy depends only logarithmically on M_A

$$\delta y = \ln \frac{M_A}{2E_{e,beam}} \tag{4}$$

  where $E_{e,beam}$ is the electron beam energy. This function is shown in figure Fig. 6 as a dashed line, and gives a maximum rapidity boost of 1.7. The decay products of this particle A are typically centred in 1 unit of pseudorapidity around this value as is shown in Fig. 6 for three different masses for a scalar particle A. The decay products therefore are not outside the acceptance of the detector. In the case of $\tilde{e}$-$\tilde{q}$ production, M_A corresponds to the invariant mass of the $\tilde{e}$-$\tilde{q}$ system.

- For H1 the loss of acceptance will mainly influence the analysis of the forward PLUG calorimeter, which was used in [2] as a veto against energy losses close to the beam pipe. In this analysis, the cut on PLUG energies could be avoided by cutting much stronger on other quantities (θ_q). This lead to a loss of efficiency by almost a factor 2. However one should note that a reduced efficiency was anyhow expected because at much higher luminosities more and different background ($W \to e\nu$) is expected and naturally requires stronger cuts. In fact the cuts were not tuned to avoid dependencies on the forward region of the apparatus, but evolved that way naturally because the W background is strongly forward peaked.

- More uncertain is the effect of secondary interactions of particles at low angles, which hit the inner part of the magnet and produce particles at larger polar angles. Because particles at low angles tend to have very high energies at HERA, the shower products will also be highly energetic and might carry considerable transverse momentum. The net effect will be an increased energy flow for polar angles much larger than 80mrad, which could considerably disturb the measurements. At present it is not known how large the effects will be on average, and more important here, to what extend tails in the $P_{T,miss}$ distribution would be induced. If this turns out to be the case, then such secondary interactions must be tagged in order to maintain the present situation of an almost background free signal.

In conclusion, there is no direct loss of acceptance for new particle searches. It remains however to be proven that the tails of the $P_{T,miss}$ distributions from SM processes can be controlled. In any case, one should not use a reduced detector performance for new particles searches as an argument against a luminosity upgrade. In contrast, only a major increase of the luminosity, far beyond 100 pb^{-1} per experiment, allows also for the future the possibility of discoveries at HERA.

9 Summary

The process $eq \to \tilde{e}\tilde{q} \to e\chi_1^0 q\chi_1^0$ was found to yield a very clean signal for Supersymmetry at HERA. With simple kinematic cuts on missing momenta and angular distributions the background from Standard Model processes can be reduced down to 0.16 events expected events from $W \to e\nu$ for an integrated luminosity of 500 pb^{-1}. It is argued that these results are also realistic for a detector setup with magnets close to the interaction vertex.

For a photino like χ_1^0, masses up to $(M_{\tilde{e}} + M_{\tilde{q}})/2 \lesssim 100$ GeV can be explored for $M_{\chi_1^0} \lesssim 75$ GeV with only minor dependences on other parameters of the MSSM. No assumptions on constraints from GUT models are made here. Similar values for $M_{\tilde{e},\tilde{q}}$ can be reached in a high luminosity run at LEP2, however with different dependences on the parameters of the MSSM. Results from the Tevatron experiments exclude much larger squark masses. These bounds are however at present not valid for large gluino masses or heavy χ_1^0's, and have been derived with different theoretical assumptions. It seems plausible that also in the future a gap for HERA might remain in case the χ_1^0 mass is close to the squark mass.

It has to be emphasised that the HERA results are only limited by statistics, and that either with an increase of the integrated luminosity or, even more favourable, with an increase of the beam energies, this search could carry on to even higher masses.

Acknowledgment

I would like to thank Herbi Dreiner for his careful reading of the manuscript as well as for his stimulation during the workshop.

References

[1] H.P.Nilles, Phys. Rep. **110** (1984) 1.
H.Haber and G.Kane, Phys. Rep. **C117** (1985) 75.
G.G.Ross, *Grand Unified Theories*, Benjamin Cummings (1985).
for a recent review see H. Baer et. al.,
FSU-HEP-950401, hep-ph/953479, and references therein.

[2] H1 Collaboration, S. Aid et al., Phys. Lett. B380 (1996) 461.

[3] H. Dreiner, P. Morawitz, Nucl. Phys. B428 (1994) 31.

[4] D. Graudenz, K. Meier, O. Nachtmann, D. Stevens, K. Zuber, these proceedings.
M. David, these proceedings.

[5] M. Corradi, these proceedings.

[6] J. Bartels, W. Hollik, Z. Phys. C39 (1988) 433.

[7] H. Baer, F. Paige, S. Protopopescu and X. Tata, Proceedings of the workshop on Physics at Current Accelerators and Supercolliders, ed. J. Hewett, A. White and D. Zeppenfeld, Argonne National Laboratory (1993).

[8] T. Sjöstrand, Comp. Phys. Comm. **82** (1994) 74.

[9] W. de Boer, Prog. Part. Nucl. Phys. **33** (1994) 201-302.

[10] Proceedings of the workshop on 'Physics at LEP 2', ed. G. Altarelli, T. Sjöstrand and F. Zwirner, Geneva 1996.

[11] CDF Collaboration, F. Abe et al., Phys. Rev. Lett. **69** (1992) 3439.
D0 Collaboration, S. Abachi et al., Phys. Rev. Lett. **75** (1995) 618.
CDF Collaboration, F. Abe et al., Phys. Rev. Lett. **76** (1996) 2006.